NON-LINEAR MECHANICAL RESPONSE OF TRIAXIAL BRAIDED COMPOSITES UNDER TENSION

T. Wehrkamp-Richter[*1,2], S. T. Pinho[2], R. Hinterhölzl[1]

[1]*Institute for Carbon Composites, Technische Universität München, Faculty of Mechanical Engineering, Boltzmannstrasse 15, D-85478 Garching b. München, Germany*
[2]*Department of Aeronautics, Imperial College London, South Kensington Campus, London SW7 2AZ, UK*
[*] *Corresponding Author: wehrkamp-richter@lcc.mw.tum.de*

Keywords: Textile composites, Damage mechanics, Digital image correlation

Abstract
The presented work investigates the non-linear mechanical response of different 2×2 triaxial braided composites under multi-axial loading. Straight-sided specimens were subjected to incremental tensile load cycles, which included loading, unloading and reloading up to final failure. This procedure allows characterizing the evolution of plastic strain and damage and hence provides an insight into the physical phenomena acting within the material. A total of three braid architectures were investigated, comprising braiding angles of 30°*,* 45° *and* 60° *loaded in the axial and transverse direction. Digital image correlation (DIC) was used to identify and locate constituent failure mechanisms and investigate surface crack propagation. Micro-sections of the specimen were analysed for the purpose of geometrical material characterization and assessment of failure mechanisms in the thickness direction.*

1. Introduction

Applying new lightweight materials such as carbon fibre reinforced plastics in the automotive industry allows a significant reduction in structural weight and carbon dioxide emissions. In these high-volume production industries, current manufacturing technologies face a twofold challenge: cost and cycle time. Braiding combines an automated and reproducible process together with an excellent rate of material deposition for mass-production of high performance structures. Yarns of several thousand carbon fibres are intertwined and positioned on a mandrel to produce geometries with complex cross-sections. Triaxial braids comprise an integrated structure of yarns oriented in three in-plane directions, which makes them a well-suited choice for multi-axial loading. Their natural through-thickness reinforcement provides excellent specific energy absorption characteristics in combination with a high degree of delamination resistance. Mechanical in-plane properties, however, suffer from the textile nature of braids, as the intertwining yarns inevitably exhibit a certain degree of out-of-plane and in-plane waviness. Hence, a reduction of stiffness and strength can be observed relative to unidirectional composites. The inherent textile nature, which includes a multitude of curved yarn interfaces, resin rich areas and nesting of multiple plies, yields a complex damage and failure behaviour. Macroscopically, a non-linear constitutive response may be observed, with the non-linearity being due to a combination of a damage and plasticity.

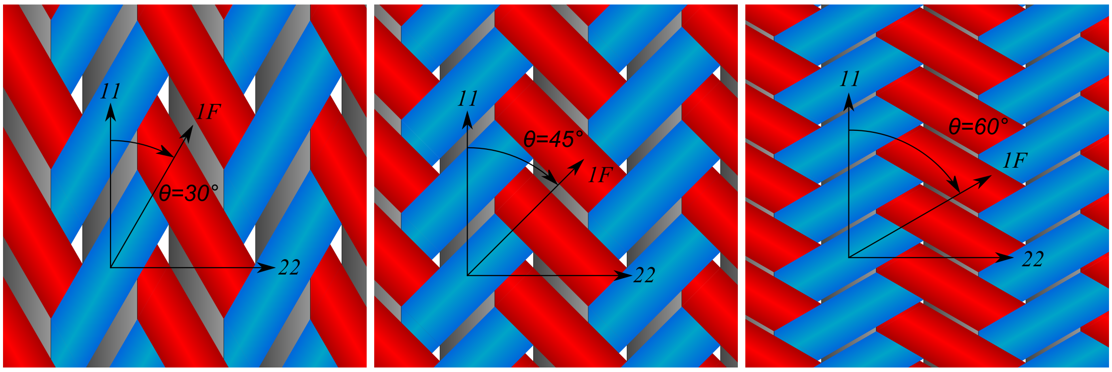

(a) [0/±30] (b) [0/±45] (c) [0/±60]

Figure 1: Triaxial braid architectures under investigation

This experimental work investigates the non-linear mechanical response of different braid architectures under multi-axial loading. For this purpose, straight-sided specimens were subjected to incremental tensile load cycles, which included loading, unloading and reloading up to final failure. Following the approach described by Ladeveze and Le Dantec [1], the evolution of plastic strain and damage provides an insight into the physical phenomena acting within the material. A total of three two-dimensional 2×2 braid architectures were investigated, comprising braiding angles of 30°, 45° and 60°. Multi-axial stress states were achieved as a result of off-axis testing in each respective braid take-up (11) and transverse direction (22). The described architectures are displayed in Fig. 1, where θ denotes the braiding angle. DIC was used to obtain the strain field, identify and locate constituent failure mechanisms and investigate surface crack propagation. Micro-sections of the specimen were analysed for the purpose of geometrical material characterization and assessment of failure mechanisms in the thickness direction.

2. Experiments

2.1. Materials

The materials investigated in this study feature 2D 2x2 triaxial braided preforms manufactured from Toho-Tenax HTS40 F13 12K yarns for both the axial (11) and braid yarn direction (1F) in combination with a Hexcel Hexflow RTM6 epoxy resin. All three braid architectures, with a nominal braiding angle of 30°, 45°, and 60°, were manufactured on a radial braiding machine with 176 bobbins. Single layers of triaxial braid were produced by over-braiding on a cylindrical mandrel, which was guided through the braiding point by a robot at constant axial take-up speed. For each braiding angle, a different mandrel diameter was used in order to obtain full fibre coverage. As a result, similar fibre areal weights were achieved, which allows a comparison of different braiding angles. Machine parameters were optimized such that the yarn dimensions of all braid architectures match as closely as possible. In order to produce flat panels, each braid layer was cut along the axial yarn direction, removed from the mandrel and subsequently flattened. Composite plates were produced with a total of four triaxial braid plies each. For resin infusion, the vacuum assisted process (VAP) technology was selected to minimize void content and to yield similar fibre volume fractions in all plates as a result of constant compaction pressure. The resin system for all braid architectures consisted of a Hexcel HexFlow RTM 6 resin. This matrix material is a one-part untoughened 180°C cure epoxy system designed for the RTM process. Fibre volume fractions for each panel were obtained from three locations using an acid digestion technique. The [0/±30] braid architecture panels had an average fibre volume fraction of 58%, the [0/±45] 56% and the [0/±60] 57%.

2.2. Test set-up

All cyclic tensile tests were performed according to ASTM D3039. A specimen width of 25 mm was selected in order to cover a minimum of two unit cells, as defined by [2]. In general, all tests were carried out under displacement control. A maximum of seven loading, unloading and reloading cycles were selected, in order to avoid the possibility of low-cycle fatigue phenomena [1]. The final reloading cycle caused failure of the specimen. Unloading was carried out at specified load levels. A displacement defined load state was chosen for the [0/±30] braid architecture due to its plateau like material response of the under transverse tension. The load levels were determined to correspond specifically with transition regions in the material response. These regions of interest were identified in preliminary monotonic tensile tests.

An electromechanical *Hegewald&Peschke* testing machine with hydraulic grips capable of loading 250 kN was operated with a head speed of 2 mm/min. For proper load introduction, fibre glass fabric tabs of 50 mm length were bonded to the specimen grip region, leaving a total gage length of 150 mm. Full field measurement of surface strains was undertaken using the commercial DIC system GOM ARAMIS in 3D mode with a maximum camera resolution of 4 MP. A comprehensive description of DIC can be found in [3]. The field of view was centred at the coupon midpoint and covered approximately 70 mm of the gage length and the entire specimen width. Average stress-strain curves were generated by averaging the entire surface strain field.

2.3. Experimental Methodology

Damage was characterized in terms of a macroscopic modulus degradation for each orthotropic braided composite architecture. The scalar damage variable d according to [1] was obtained after each unloading cycle as

$$d_i = 1 - \frac{E_i}{E_0} \tag{1}$$

where E_i is the unloading secant modulus calculated from the end points of the loading and unloading part of cycle i and E_0 is the elastic modulus calculated from a moving least squares fit in cycle 1. The accumulated inelastic strain component $\varepsilon_{pl,i}$ was determined from

$$\varepsilon_{pl,i} = \varepsilon_i - \frac{\sigma_i}{E_i} \tag{2}$$

where the measured scalar damage variable and the inelastic residual strain represent homogenised material quantities caused by a combination of failure modes occurring within a triaxial braided composite, such as inter-yarn and intra-yarn matrix failure, delaminations, progressive fibre failure and fibre-matrix debonding.

3. Results and discussion

Representative cyclic stress-strain curves for all test cases are displayed in Fig. 2. The evolution of the scalar damage variable d and the plastic strain ε_{pl} are shown in Fig. 3 and Fig. 4 as a function of total strain, respectively. For each braid architecture, a polynomial fit illustrates the average evolution of both variables up to the corresponding failure strain.

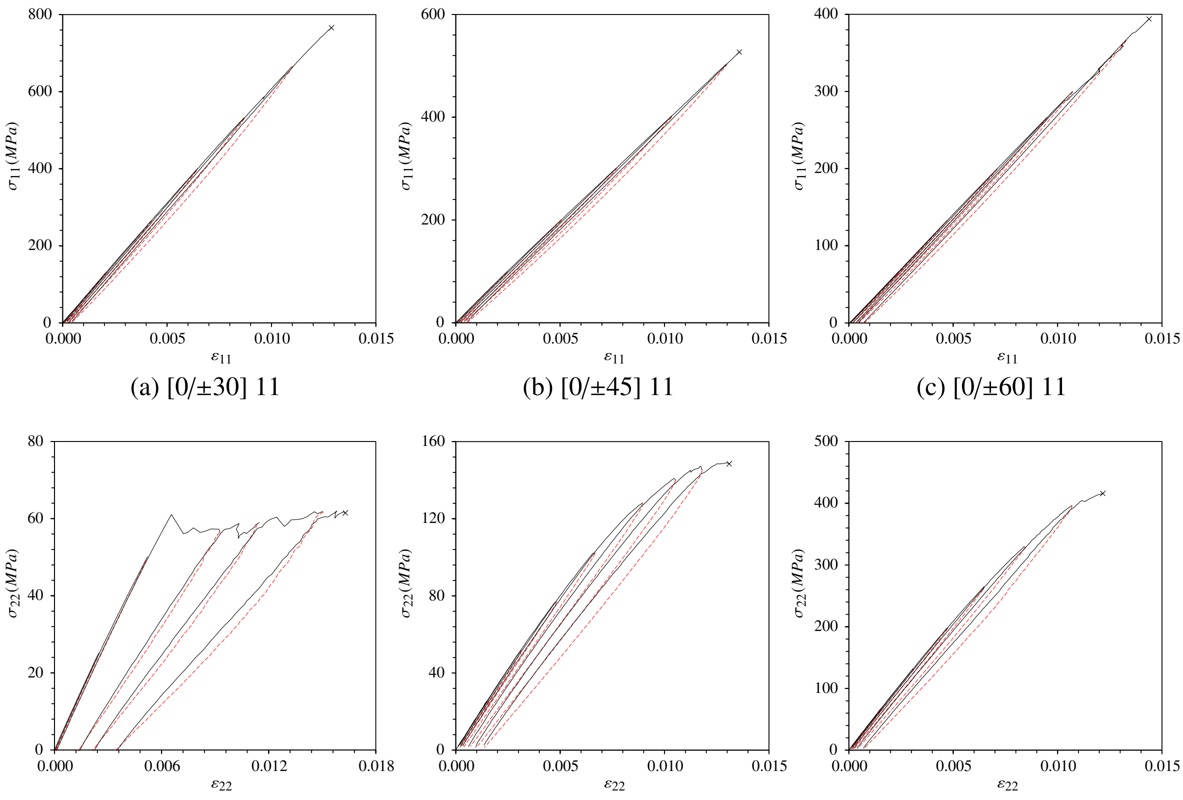

(a) [0/±30] 11 (b) [0/±45] 11 (c) [0/±60] 11

(d) [0/±30] 22 (e) [0/±45] 22 (f) [0/±60] 22

Figure 2: Representative stress-strain curves for loading parts (black) and unloading parts (red) of all cycles

3.1. Loading in 11 Direction

For the cases in which the load is aligned with the axial fibre direction (11), only minor non-linearities are present in the material, independently of the braiding angle. The damage variable for the [0/±30] and the [0/±45] braided composite remains at a steady level below 5%. In this range, the experimental data exhibits a larger scatter. One possible explanation for this phenomenon is the higher impact of noise from the DIC system when measuring very small strains, which can cause minor differences between the initial and subsequent modulus measurements. For both test cases, the surface strain fields indicate strain concentrations located at the lateral yarn interfaces, but no macroscopic cracks are evident throughout the loading history. The plastic strain shows a gradual increase. However, considering a maximum of 0.05% at an average

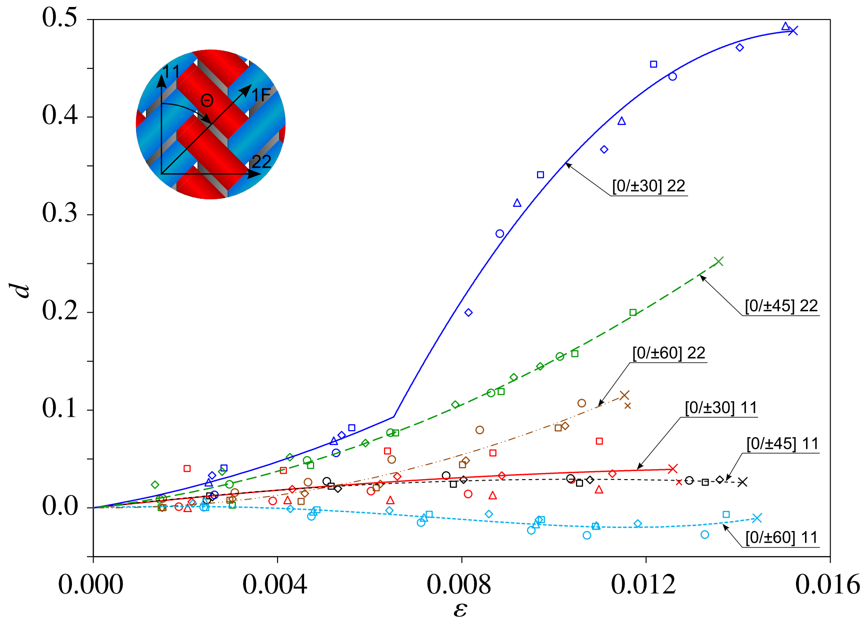

Figure 3: Evolution of the scalar damage variable *d*

failure strain of about 1.3%, the total contribution for all braid architectures in 11 direction remains negligible.

The [0/±60] architecture shows a stiffening effect upon loading, indicated by a negative damage variable, which is caused by a combination of axial yarns straightening and braid yarn alignment in load direction. At an applied stress of approximately 300 MPa, a sudden decrease of the tangent modulus is observed. This point corresponds to the first localized cracks appearing on the specimen surface both at the interface and inside adjacent braid yarns, indicating inter- and intra-yarn matrix cracking. When the load is further increased within a cycle, these cracks propagate along the braid fibre direction, until they are arrested by an intersecting braid yarn. An increase in applied stress allows further crack growth along the intersecting braid yarn direction, thus forming a zigzag crack pattern over the entire specimen width. This process continues, until the entire specimen is saturated with cracks. Although this phenomenon yields at first a decrease in tangent modulus, it is followed by a gradual stiffening process. It appears that the formation of multiple cracks removes constraints in the material, which allows further alignment of the braid yarns and straightening of the axial yarns in the load direction, resulting in an increase in stiffness. When unloading occurs after the process has finished, no significant increase in the damage variable could be observed.

3.2. Loading in 22 direction

Significant non-linearities occur for loading in the transverse direction. For the [0/±60] braided composite, the accumulated plastic strain before final failure is comparable to the 11 test cases, even if the corresponding failure strain of 1.2% is slightly lower. The damage variable shows a gradual increase to approximately 10% at final failure. The experimental data suggests that damage is primarily driven by intra-yarn matrix cracking of the axial yarns loaded in transverse tension. At about half the failure strain, these cracks manifest on the surface as strain concentrations located at the positions of underlying axial yarns. However, this mechanism results in a

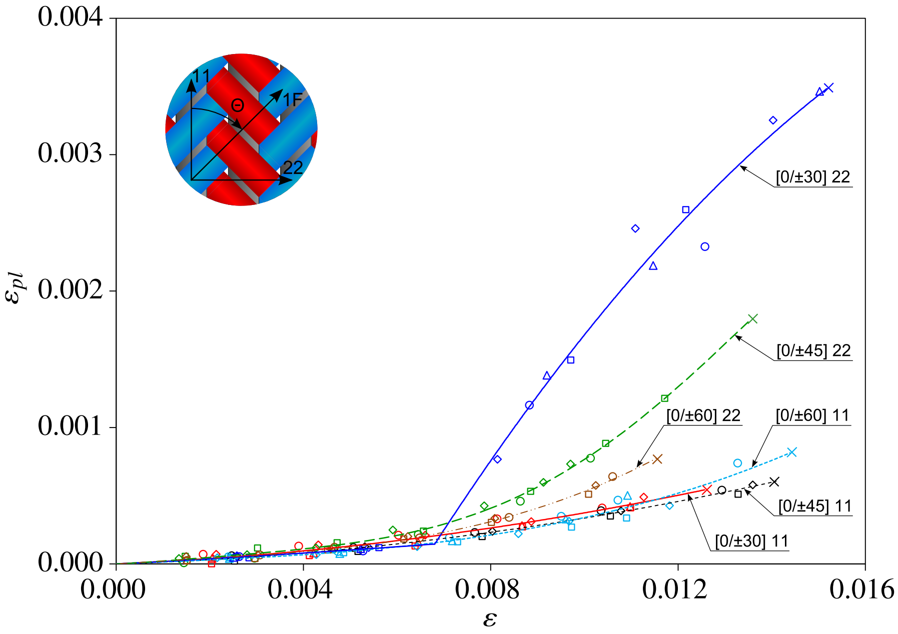

Figure 4: Evolution of plastic strain ε_{pl}

limited gradual modulus degradation, since loads can be redistributed to the braid yarns, which prevent catastrophic failure.

In the [0/±45] braid, both the stiffness degradation and plastic strains play an important role in the non-linear mechanical response. Here, the surface strain field capture intra-yarn matrix cracks in both the braid yarns and the axial yarns. The presence of small gaps between adjacent braid yarns reveals regions of split axial yarns in this architecture. The braid yarns are directly loaded in shear, which might contribute significantly to the evolution of plastic strains.

The mechanical response of the [0/±30] can be separated into two distinct domains up to final failure. In the first domain, the highest gradual increase in damage out of all architectures is accompanied by a negligible increase in plastic strain. Strain concentrations arise at the yarn interfaces, but no macroscopic cracks are visible on the specimen surface. When a critical load level is reached, inter-yarn cracks form at the boundaries of adjacent yarns at a specific location across the specimen length. Their initial appearance can be correlated with the first major load drop. As the strain further increases, the load level exhibits a stable plateau as a result of progressive cracking in the axial and braid yarns. In contrast to the [0/±60] and [0/±45] architecture, the surrounding braid yarns are not capable of recovering major parts of the redistributed stresses during an axial yarn failure. In addition, the bias angle of two intersecting braid yarns of 60° allows cracks to propagate over the specimen width more easily. Before final failure of the specimen, the modulus has significantly degraded to almost 50% of its initial value, with a considerable inelastic strain of 0.35%.

4. Conclusion and Outlook

This paper investigated the non-linear mechanical response of different 2×2 triaxial braided composites under tensile load. Whereas only minor non-linearities were present for loading in the axial yarn direction, severe non-linearities could be observed for the transverse load case.

The mechanical response was found to be largely dominated by the textile architecture, which significantly affects localisation, crack propagation and load redistribution in the material. The formation of inter-yarn and intra-yarn cracks could be correlated with damage and irreversible strains in the material. This information shall serve as baseline for the development of a numerical model for predicting the non-linear constitutive behaviour of triaxial braided composites.

5. Acknowledgements

The presented paper was initiated by an international joint research program of the Korea Institute of Carbon Convergence Technology (KCTECH), Doolim Robotics and the Institute for Carbon Composites (LCC) at Technische Universität München. This work was supported by the Ministry of Trade, Industry and Energy (MOTIE) in Korea through the international joint research program. The first author acknowledges the support provided by Dr. Markus G. R. Sause at the University of Augsburg.

References

[1] P. Ladeveze and E. Le Dantec. Damage modelling of the elementary ply for laminated composites. *Composites Science and Technology*, 43(3):257–267, 1992.

[2] P. J. Minguet, M. J. Fedro, and C. K. Gunther. Test Methods for Textile Composites: NASA Contractor Report 4609. 1994.

[3] B. Pan, K. Qian, H. Xie, and A. Asundi. Two-dimensional digital image correlation for in-plane displacement and strain measurement: a review. *Measurement Science and Technology*, 20(6):062001, 2009.